

This article was downloaded by:

On: 28 January 2011

Access details: *Access Details: Free Access*

Publisher *Taylor & Francis*

Informa Ltd Registered in England and Wales Registered Number: 1072954 Registered office: Mortimer House, 37-41 Mortimer Street, London W1T 3JH, UK



Physics and Chemistry of Liquids

Publication details, including instructions for authors and subscription information:

<http://www.informaworld.com/smpp/title~content=t713646857>

Dynamical Properties of Liquid Binary Alloys: A Memory Function Study

Ya. Chushak^{ab}; T. Bryk^{ab}; A. Baumketner^a; G. Kahl^b; J. Hafner^b

^a Institute for Condensed Matter Physics, National Ukrainian Academy of Sciences, Lviv, Ukraine ^b

Institut für Theoretische Physik and CMS, Wien, Austria

To cite this Article Chushak, Ya. , Bryk, T. , Baumketner, A. , Kahl, G. and Hafner, J.(1996) 'Dynamical Properties of Liquid Binary Alloys: A Memory Function Study', *Physics and Chemistry of Liquids*, 32: 2, 87 – 102

To link to this Article: DOI: 10.1080/00319109608030709

URL: <http://dx.doi.org/10.1080/00319109608030709>

PLEASE SCROLL DOWN FOR ARTICLE

Full terms and conditions of use: <http://www.informaworld.com/terms-and-conditions-of-access.pdf>

This article may be used for research, teaching and private study purposes. Any substantial or systematic reproduction, re-distribution, re-selling, loan or sub-licensing, systematic supply or distribution in any form to anyone is expressly forbidden.

The publisher does not give any warranty express or implied or make any representation that the contents will be complete or accurate or up to date. The accuracy of any instructions, formulae and drug doses should be independently verified with primary sources. The publisher shall not be liable for any loss, actions, claims, proceedings, demand or costs or damages whatsoever or howsoever caused arising directly or indirectly in connection with or arising out of the use of this material.

DYNAMICAL PROPERTIES OF LIQUID BINARY ALLOYS: A MEMORY FUNCTION STUDY

YA. CHUSHAK^{1,2}, T. BRYK^{1,2}, A. BAUMKETNER¹,
G. KAHL² and J. HAFNER²

¹*Institute for Condensed Matter Physics, National Ukrainian Academy
of Sciences, 1 Svientsitsky St., Lviv 290011, Ukraine*

²*Institut für Theoretische Physik and CMS, TU Wien, Wiedner
Hauptstraße 8-10, A-1040 Wien, Austria*

(Received 18 December 1995)

The dynamical properties of binary liquid mixtures are investigated within a viscoelastic model using the memory function approach. Extending the viscoelastic model to the binary case we find that the dynamical properties of the liquid mixture are characterized by four propagating and two diffusive modes. We show that the character of the two propagating modes depends strongly on the relative concentration of the light and heavy atoms, in close analogy to the vibrational eigenmodes in substitutionally disordered crystalline and glassy mixtures. The relation of these two eigenmodes to the “fast sound” phenomenon observed in mixtures with strongly different masses is discussed.

KEY WORDS: Viscoelastic model, Langevin equations.

1. INTRODUCTION

During the past decade the study of the dynamical properties of liquid metals has been the subject of numerous theoretical and experimental investigations (see, e.g.,¹ for an overview). Much less attention has been devoted to the microscopic dynamics of liquid alloys. Ever since the first theoretical study of the collective excitations in a liquid Na_{0.5}K_{0.5} alloy² only a few further experimental³ and theoretical investigations (by means of computer simulations)^{4–6} have been performed. Among these one of the most significant results has been obtained by Bosse *et al.*⁶ in a molecular-dynamics (MD) study of a liquid Li_{0.7}Pb_{0.3} alloy where a new high-frequency collective mode at long wavelengths (“fast sound”) was found. Meanwhile such modes were also observed in other systems (such as water⁷, He-Ne mixtures⁸ or liquid Li₄Tl and Li₄Pb alloys⁹). The crucial parameter for the appearance of such a phenomenon are disparate masses. The appearance of a second “second” mode differs from what is expected in the hydrodynamic approximation, where only one sound propagation frequency is predicted. The pioneering studies of the fast sound phenomenon were based on an analysis of the dynamic structure factors obtained from the inelastic scattering experiment and from MD simulation: the dynamic structure factors $S(k, \omega)$ are fitted by a linear combination of Lorentzians⁸. It turns out that a minimum number of four Lorentzians centered at $\pm \omega_s^{(j)}(k)$, $j = 1, 2$ is

needed for an accurate fit. The higher-lying eigenmode at a frequency $\omega_s^{(1)}(k) > ck$ (where c stands for the velocity of sound) is visible in $S(k, \omega)$. It can be associated with the motion of the lighter particles and represents the fast sound mode: this mode is virtually identically with the hydrodynamic sound mode in a fluid consisting of the lighter particles only. The mode with $\omega_s^{(2)}(k) < ck$ is not directly visible in $S(k, \omega)$, it corresponds to slow motions of the heavier particles. These results have been analyzed in a kinetic model (hard-sphere mixtures and in the dense-fluid and gas states)¹⁰⁻¹³ which predicts that the fast sound vanishes at very long wavelength and that the slow sound merges with the hydrodynamic sound mode in this range.

In this paper we want to investigate whether the fast sound phenomenon is also relevant for understanding the dynamical properties of liquid metal alloys with a moderate to large difference in the atomic masses. Our approach to describe the dynamics of liquids is based on the viscoelastic model using the memory function approach¹⁴. As found in a large number of studies a simple exponential ansatz for the second order memory function can describe already fairly well the dynamic structure factor of one-component liquids in the (k, ω) -range accessible to neutron-scattering experiment. We have recently used the viscoelastic model to analyze the complex structures of the molten metallic state of the semiconductor Ge and the molten semimetal As¹⁵.

In this contribution we extend the memory function framework to study the dynamic structure factor of liquid binary alloys. We truncate the (generalized) continued fraction expansion of the intermediate scattering functions $F_{ij}(k, t)$ at the level of the second order memory function (as usually done in the one-component case) and thus yield approximate expressions for the $F_{ij}(k, t)$ corresponding to those obtained in the one-component case from the three-pole approximation proposed by Lovesey¹⁶. This model allows a direct calculation of the dispersion relations and of the half-widths of the eigenmodes from the memory functions, as well as the calculation of the partial dynamic structure factors.

The systems investigated are $K_{0.7}Cs_{0.3}$ and $K_{0.3}Cs_{0.7}$, with the mass-ratio $m_{Cs}/m_K \sim 3.4$. For both compositions the viscoelastic approach predicts six eigenmodes at each wavevector: four propagating modes with $\pm\omega_s^{(j)}$, $j = 1, 2$ and two diffusive modes. The two independent propagating modes show a characteristically different behaviour in the two alloys. At a majority composition of the lighter atoms (K) we have in zeroth order a dispersive "host" mode intersecting with a dispersionless "impurity" mode at low frequency. Around the intersection, the interaction leads to the formation of a hybridization gap. In a first approximation we can associate the two modes with "acoustic" and "optic" oscillations (with both atomic species moving in and out of phase, respectively). In the hydrodynamic regime the "optic" mode is strongly damped. At very large values of the mass ratio, the "impurity" mode drops to very low frequency. In this case the "optic" mode can be followed down to small wavevectors and becomes the fast sound mode. At a majority concentration of the heavier atoms (Cs) we have again a dominant host mode, but now an impurity mode that lies above the spectrum of the host modes. In this case the interaction is much weaker and no fast sound phenomenon can be expected. We also discuss the dynamics of the liquid alloys in relation to the dynamical properties of crystalline and glassy alloys.

The paper is organized as follows: in Sec. II we give the basic formulae of the generalized viscoelastic theory. In Sec. III we present results obtained for two liquid alkali alloys and discuss the main results in relation to the dynamics of crystalline and glassy systems in Sec. IV.

2. BASIC THEORY

The Model

We consider a binary liquid in a volume V at the temperature T , the total number density is given by ρ . Each species ($i = 1, 2$) is characterized by the number of particles N_i , the partial number densities $\rho_i = N_i/V$, the concentrations $c_i = N_i/N$, and masses m_i . The interatomic potentials are denoted by $V_{ij}(r)$ and k_B stands for the Boltzmann constant.

We define the Fourier-transform of the partial number densities as

$$\rho_k^{(j)}(t) = \frac{1}{N_j} \sum_{i=1}^{N_j} \exp[i\vec{k} \cdot \vec{r}_i^{(j)}(t)] \quad j = 1, 2. \quad (1)$$

Since we only consider spherically symmetric potentials the quantities of interest will only depend on the modulus $k = |\vec{k}|$. We are interested in the intermediate scattering function $F_{ij}(k, t)$, defined as

$$F_{ij}(k, t) = \langle \rho_k^{(i)}(t) \rho_{-k}^{(j)}(0) \rangle = [\mathbf{F}(k, t)]_{ij} \quad (2)$$

where the last equation defines the matrix $\mathbf{F}(k, t)$. The angular brackets indicate equilibrium averages. At $t = 0$, $\mathbf{F}(k, t)$ reduces to the matrix of the partial structure factors $S_{ij}(k)$

$$[\mathbf{F}(k, 0)]_{ij} = [\mathbf{S}(k)]_{ij} = S_{ij}(k). \quad (3)$$

$\mathbf{F}(k, t)$ and $\mathbf{S}(k, t)$ are symmetric. The partial dynamic structure factors $S_{ij}(k, \omega)$ are time Fourier-transforms of the corresponding intermediate scattering functions

$$S_{ij}(k, \omega) = \frac{1}{2\pi} \int_{-\infty}^{\infty} dt e^{i\omega t} F_{ij}(k, t). \quad (4)$$

Within the Mori-Zwanzig formalism¹⁴ it is straightforward to write down the generalized Langevin (or memory function) equations for the $F_{ij}(k, t)$ ¹⁷

$$\frac{d}{dt} \mathbf{F}(k, t) = - \int_0^t d\tau \mathbf{M}(k, \tau) \mathbf{F}(k, t - \tau) \quad (5)$$

where $\mathbf{M}(k, t)$ is the memory function matrix. It is convenient to introduce the Laplace-transform of the correlation functions (denoted throughout by a tilde), defined as

$$\tilde{F}_{ij}(k, z) = \int_0^\infty dt e^{-zt} F_{ij}(k, t). \quad (6)$$

Then the formal solution of Eqn. (5) is given by

$$\tilde{\mathbf{F}}(k, z) = [z\mathbf{I} + \tilde{\mathbf{M}}(k, z)]^{-1} \mathbf{F}(k, 0). \quad (7)$$

where \mathbf{I} denotes the unit matrix. It can be shown¹⁴ that the memory functions $M_{ij}(k, t)$ are themselves dynamic correlation functions; hence they satisfy an equation similar to (5) introducing the second order memory functions $N_{ij}(k, t)$ as kernel functions and the formal solution

$$\tilde{\mathbf{M}}(k, z) = [z\mathbf{I} + \tilde{\mathbf{N}}(k, z)]^{-1} \mathbf{M}(k, 0). \quad (8)$$

In principle this procedure can be continued. Due to the so-called sum-rules the initial values of the memory functions $M_{ij}(k, t=0)$ and $N_{ij}(k, t=0)$ are fixed to the frequency moments of $S_{ij}(k, \omega)$ via

$$\begin{aligned} \mathbf{M}(k, 0) &= \boldsymbol{\omega}^2(k) [\boldsymbol{\omega}_0(k)]^{-1} \\ \mathbf{N}(k, 0) &= \boldsymbol{\omega}^4(k) [\boldsymbol{\omega}^2(k)]^{-1} - \boldsymbol{\omega}^2(k) [\boldsymbol{\omega}_0(k)]^{-1} \end{aligned} \quad (9)$$

where the $\boldsymbol{\omega}^n(k)$ are the matrices of the n -th moments

$$[\boldsymbol{\omega}^n(k)]_{ij} = \langle \omega_{ij}^n(k) \rangle = \int_{-\infty}^{\infty} \omega^n S_{ij}(k, \omega) d\omega. \quad (10)$$

The required moments are given by [18]

$$\begin{aligned} \langle \omega_{ij}^0(k) \rangle &= S_{ij}(k) & \langle \omega_{ij}^2(k) \rangle &= \delta_{ij} k^2 \frac{k_B T}{m_i} \\ \langle \omega_{ij}^4(k) \rangle &= \delta_{ij} k^2 \frac{k_B T}{m_i m_j} \left(3k^2 k_B T + \sum_l \rho_e \int d\vec{r} g_{il}(r) \frac{\partial^2 V_{il}(r)}{\partial z^2} \right) \\ & - (\rho_i \rho_j)^{1/2} k^2 \frac{k_B T}{m_i m_j} \int d\vec{r} g_{ij}(r) \cos(kr) \frac{\partial^2 V_{ij}(r)}{\partial z^2}. \end{aligned} \quad (11)$$

If we introduce memory functions of order higher than two, we would need frequency moments of order six which in turn require in their explicit expressions triplet correlation functions. In this contribution we restrict ourselves—as usually done—to memory functions up to order two.

Based on this approach one can—theoretically—give exact expression for the dynamic correlation functions by means of “first principle” theories, as, e.g., the mode-coupling theory proposed by Sjögren and Sjölander¹⁹. Here we have resorted to a model by introducing an approximation at the level of the second order memory function. It is a generalization of a simple model, proposed by Lovesey for monoatomic liquids¹⁶ which has proven to give reliable results for simple liquids: in this approximation we replace the Laplace-transforms of the third-order memory functions $\tilde{K}_{ij}(k, z)$ by their values at $z = 0$

$$\tilde{\mathbf{K}}(k, z) \approx \tilde{\mathbf{K}}(k, 0) = \mathbf{K}(k), \quad (12)$$

where

$$\tilde{K}_{ij}(k, 0) = \int_0^\infty dt K_{ij}(k, t) \quad (13)$$

and hence truncate the sequence of memory functions at the level of order two. The explicit expressions for the $K_{ij}(k)$ are given at the end of this section. The second order memory functions $\tilde{N}_{ij}(k, z)$ are then obtained from the solution of the corresponding memory function equations, i.e.,

$$\tilde{\mathbf{N}}(k, z) = [z\mathbf{I} + \mathbf{K}(k)]^{-1} \mathbf{N}(k, 0). \quad (14)$$

In particular, for the component functions $N_{ij}(k, t)$ this approximation leads to an expressions which is a linear combination of two exponentials

$$N_{ij}(k, t) = \frac{b_{ij}(z_1)}{z_1 - z_2} e^{z_1 t} + \frac{b_{ij}(z_2)}{z_2 - z_1} e^{z_2 t} \quad (15)$$

where z_1 and z_2 are the roots of the equation

$$\text{Det}[z\mathbf{I} + \mathbf{K}(k)] = 0 \quad (16)$$

and

$$b_{ij}(z) = N_{ij}(k, 0)[z + K_{mm}(k)] - N_{mj}(k, 0)K_{im}(k) \quad (m = 1, 2 \text{ and } m \neq i). \quad (17)$$

We want to point out that within this model the $F_{ij}(k, t)$ (and hence the $S_{ij}(t, \omega)$) satisfy the sum-rules up to order four irrespective of the choice of $\tilde{\mathbf{K}}(k, z)$.

From equations (8) and (14) we find that $\mathbf{K}(k)$ is related to $M_{ij}(k, t)$ via

$$\mathbf{K}(k) = \mathbf{N}(k, 0)\tilde{\mathbf{M}}(k, z=0)\mathbf{M}^{-1}(k, 0) \quad (18)$$

where

$$\tilde{M}_{ij}(k, 0) = \int_0^\infty dt M_{ij}(k, t). \quad (19)$$

From the short-time behaviour of $M_{ij}(k, t)$,

$$\tilde{M}_{ij}(k, t) = M_{ij}(k, 0) \left[1 - \frac{1}{2} N_{ij}(k, 0) t^2 + \dots \right] \quad (20)$$

we obtain $\tilde{M}_{ij}(k, 0) = \xi M_{ij}(k, 0) \sqrt{N_{ij}(k, 0)}$ where the coefficient ξ depends on the model used for the higher-order terms.

In the limit $k \rightarrow \infty$ the $S_{ij}(k, 0)$ should converge to the free-gas result where

$$S_{ij}(k, 0) = \delta_{ij} \left(\frac{1}{2\pi k^2} \frac{m_i}{k_B T} \right)^{1/2} \quad (21)$$

and $\mathbf{M}(k, 0)$ and $\tilde{\mathbf{M}}(k, 0)$ become diagonal matrices. It is easy to show that the above free-gas limit is obtained if $\xi = 2/\pi$ and

$$K_{ii}(k) = \frac{2}{\sqrt{\pi}} \sqrt{N_{ii}(k, 0)}$$

$$K_{ij}(k) = \frac{2}{\sqrt{\pi}} \frac{N_{ij}(k, 0)}{\sqrt{N_{ij}(k, 0)}} \quad \text{for } i \neq j. \quad (23)$$

The $K_{ii}(k)$ have the same functional form as encountered in Lovesey's model¹⁶ for simple liquids.

Based on this model the dispersion relations $\omega_s(k) = iz(k)$ are obtained as the solutions of the equations

$$\text{Det} [z\mathbf{I} + \tilde{\mathbf{M}}(k, z)] = 0 \quad (24)$$

which in our approach reduces to an equation of order six in z . These roots correspond to six modes: two of them ($j=3, 4$) turn out to be real, i.e., they describe purely diffusive (non-propagating) processes. The remaining four roots are two pairs of complex conjugate roots [$z^{(j)}(k) = -\Gamma^{(j)}(k) \pm i\omega_s^{(j)}(k)$, $j=1, 2$]: they represent the dispersions $\omega_s^{(j)}(k)$ and the sound damping coefficients $\Gamma^{(j)}(k)$.

In literature, very frequently the position of the main peak in the longitudinal current correlation function $C_l(k, \omega)/C_{l,ij}(k, \omega)$ as a function of k is also called dispersion relation, which we will denote in this contribution by $\omega_l(k)/\omega_l^{ij}(k)$. Since $C_l(k, \omega) = (\omega^2/k^2)S(k, \omega)$ and since the dynamic structure factor is easily accessible from our model, we will also compare the $\omega_l(k)$'s with $\omega_s^{(j)}(k)$.

The total neutron-weighted dynamic structure factor $S(k, \omega)$ is obtained from the partials $S_{ij}(k, \omega)$ by means of the standard relation

$$S(k, \omega) = c_1 \bar{b}_1^2 S_{11}(k, \omega) + c_2 \bar{b}_2^2 S_{22}(k, \omega) + 2\sqrt{c_1 c_2} \bar{b}_1 \bar{b}_2 S_{12}(k, \omega) \quad (25)$$

with $\bar{b}_i = b_i / \sqrt{c_2 b_1^2 + c_2 b_2^2}$, $i=1, 2$ where b_i are the scattering lengths for species i (taken from²⁰).

The Static Structure

The interatomic potentials are calculated from simple Ashcroft “empty-core” pseudopotentials²¹ using the dielectric screening function with the local-field corrections proposed by Ichimaru and Utsumi²². For more details about the construction of the effective pair potentials for binary alloys we refer the reader to²³.

The static structure of the binary alloys investigated has been determined both in MD simulations as well as by means of integral-equations techniques. The simulations have been performed using a standard micro-canonical simulations technique for 4000 particle ensemble. The static structure functions were obtained as averages over 20 000 time-steps. Details about the integral-equation technique are given elsewhere²⁴; it is based on a universal modeling of the bridge-functional²⁵ and has led for a large variety of systems to very satisfactory results. The partial static structure factors for $K_{0.7}Cs_{0.3}$ are shown in Figure 1. Agreement between the MD simulation and the integral-equation results turns out to be very satisfactory. Based on the static structure and the interatomic potentials the moments $\omega^n(k)$ have been calculated using the standard expressions listed above.

3. RESULTS

We have studied the dynamical properties for two liquid binary alkali alloys by means of the model outlined above: $K_{0.7}Cs_{0.3}$ ($\rho = 0.01083 \text{ \AA}^{-3}$) and $K_{0.3}Cs_{0.7}$ ($\rho = 0.0091 \text{ \AA}^{-3}$), both at a temperature of 373 K.

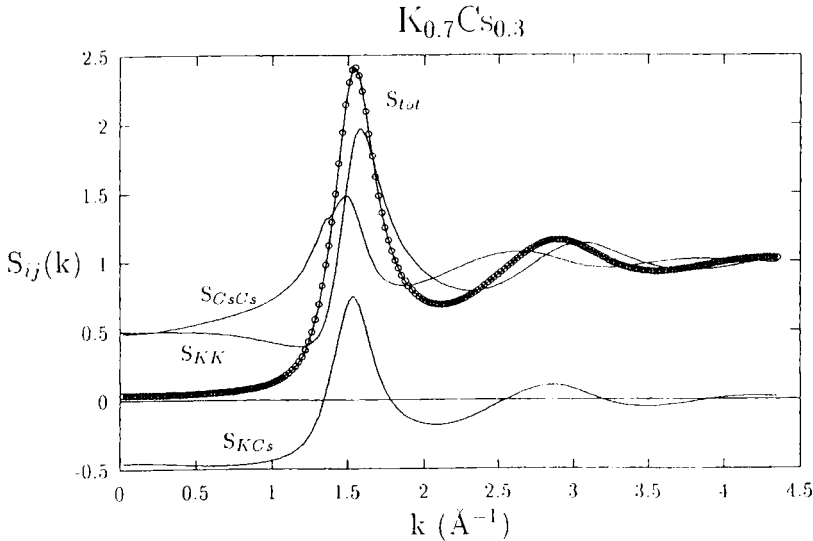


Figure 1 Partial static structure factors $S_{ij}(k)$ for a $K_{0.7}Cs_{0.3}$ alloys and total structure factor $S(k)$ as labeled as obtained from the integral-equation approach.

Figure 2 shows the dispersion relations $\omega^{(j)}(k), j = 1, 2$ (i.e., the two roots of the propagating modes according to Eqn. (24) for the two alloys considered in this study. Furthermore we have depicted the dispersion relations calculated for the pure elements K and Cs within the same method at the same temperature. This comparison shows that the low-energy mode is essentially determined by the motions of the heavier atoms. However, whereas at a majority concentration of the heavy atoms it follows closely the dispersion law of pure liquid Cs with a dispersion-minimum close to the position of the first peak in the static structure factor (cf. Fig. 1), at a majority concentration of the lighter atoms the mode follows the sound-wave dispersion only at small k and shows little dispersion at larger wavevectors. The high-energy mode has a finite frequency at $k = 0$ (like an optic mode in a crystal) and follows the dispersion law of the lighter species at larger k . The dispersion is strongly reduced if the lighter atoms are the minority species.

In Figures 3 and 4 we display the two dispersion relations $\omega_s^{(j)}(k), j = 1, 2$ along with the dispersion relations $\omega_l^{ij}(k)$ ($i, j = K, Cs$) obtained from the positions of the main peaks of the partial current-correlation functions $C_l^{ij}(k, \omega) = (\omega^2/k^2)S_{ij}(k, \omega)$. Figure 3 shows the results for the K-rich alloy, Figure 4 for the Cs-rich system. In both cases $\omega_l^{CsCs}(k)$ follows closely the low-frequency dispersion $\omega_s^{(2)}(k)$, while $\omega_l^{KK}(k)$ merges for intermediate k 's with the high-frequency mode $\omega_s^{(1)}(k)$. Differences between $\omega_l^{KK}(k)$ and $\omega_s^{(1)}(k)$ are observed in particular for small k 's where $\omega_s^{(1)}(k)$ tends to a finite frequency as the optic modes in a crystal. A further characteristic difference between the high-frequency propagating mode and the other modes appears

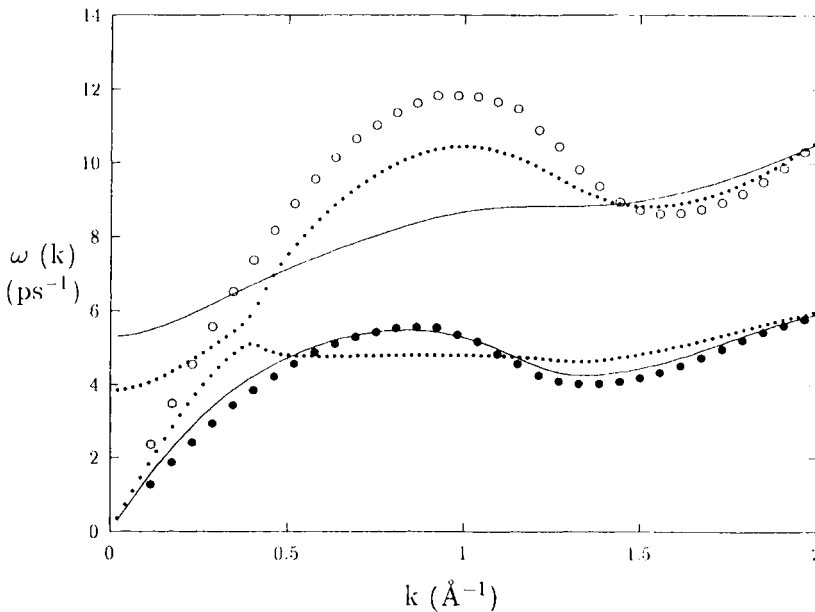


Figure 2 Dispersion relations $\omega^{(j)}(k), j = 1, 2$ for the two binary alloys studied along with the dispersion relations $\omega_s^{ij}(k)$ for the pure metals. Symbols: open circles—pure K, full circles—pure Cs; full lines— $K_{0.3}Cs_{0.7}$, dotted lines— $K_{0.7}Cs_{0.3}$; the upper (lower) curves correspond to $j = 1(2)$.

Downloaded At: 08:12 28 January 2011

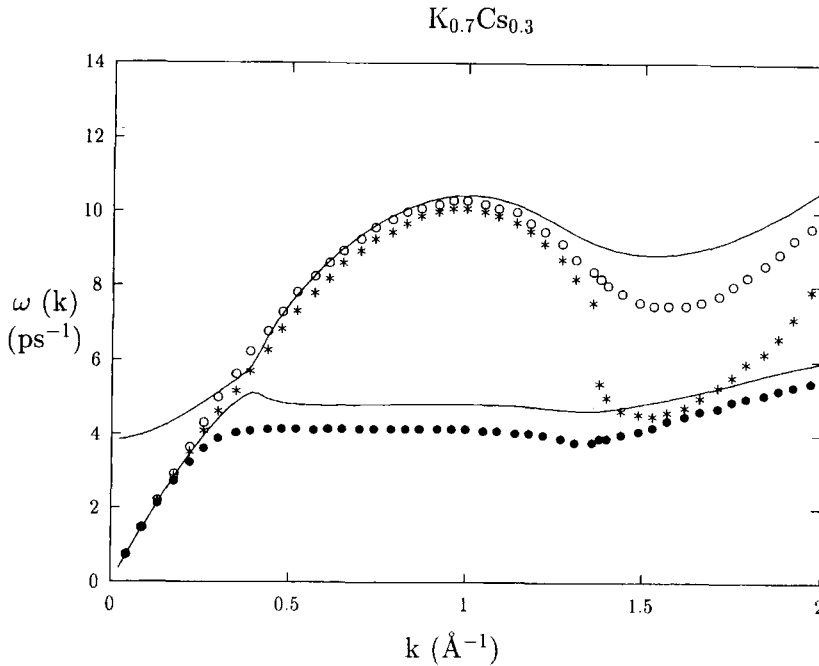


Figure 3 Dispersion relations $\omega_j^{(j)}(k)$, $j = 1, 2$ for the $K_{0.7}Cs_{0.3}$ alloy ($j = 1$ – upper full curve, $j = 2$ – lower full curve) along with the dispersion relation $\omega_l^{(j)}(k)$ derived from the positions of the peak in the total and partial longitudinal current-correlation functions $\omega^2 S(k, \omega)/k^2$ (*), $\omega^2 S_{KK}(k, \omega)/k^2$ (o) and $\omega^2 S_{CsCs}(k, \omega)/k^2$ (●); ('1' = K and '2' = Cs).

when we consider the damping coefficients $\Gamma^{(j)}(k)$, defined as the real parts of the roots $z^{(j)}$ of Eqn. (24), displayed in Figure 5 and 6. In contrast to the other modes (including also the non-propagating modes $z^{(j)}(k)$, $k = 3, 4$, i.e., the purely real roots) the damping of the high-frequency mode is in particular strong at low k . It increases with decreasing k and remains non-zero for $k = 0$. For all other modes the damping goes to zero in the limit $k = 0$. The strong overdamping of the high-frequency mode (or fast sound) was also observed in hard-sphere mixtures by Campa and Cohen¹². The characteristic difference between the two alloys is that the interaction between the low and high-frequency modes is strong at a majority concentration of the lighter atoms whereas it is weak at a majority of the heavier atom. Where the two modes are nearly degenerate at low wavenumbers, we would expect a fast sound effect; in this range the damping of the high frequency mode is also minimal. At majority concentrations of the heavier atoms the frequencies are sufficiently different at all wavevectors, and the damping is always much stronger for the high-frequency mode than for the low-frequency mode.

Due to the strong damping, it will be rather difficult to observe the high-frequency mode experimentally. Since the scattering lengths of K and Cs are not too different ($b_K = 0.37$, $b_{Cs} = 0.55$;²⁰), the situation is relatively favourable for the K-rich alloy. Figure 7 shows the partial and the total (neutron-weighted) dynamic structure

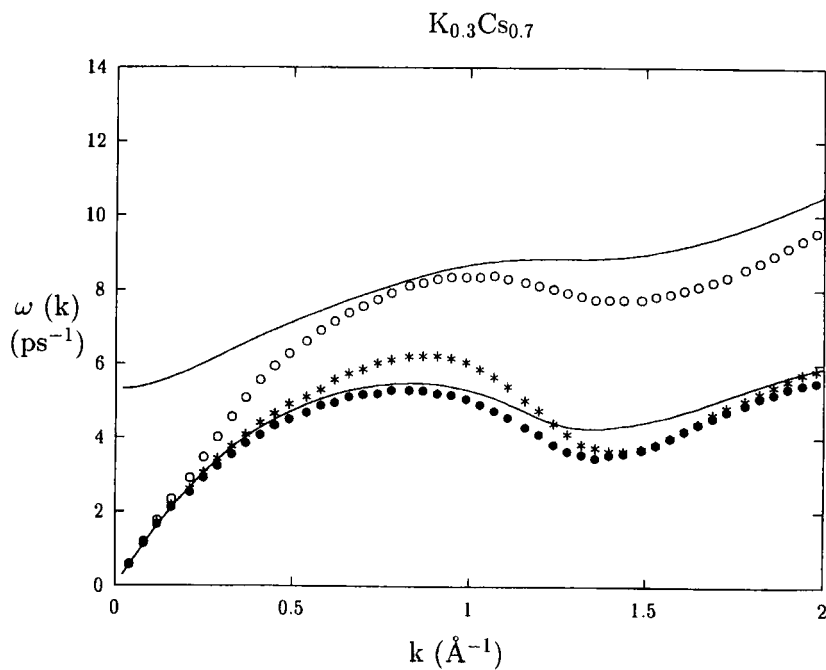


Figure 4 Same as Figure 3, but for $K_{0.3}Cs_{0.7}$.

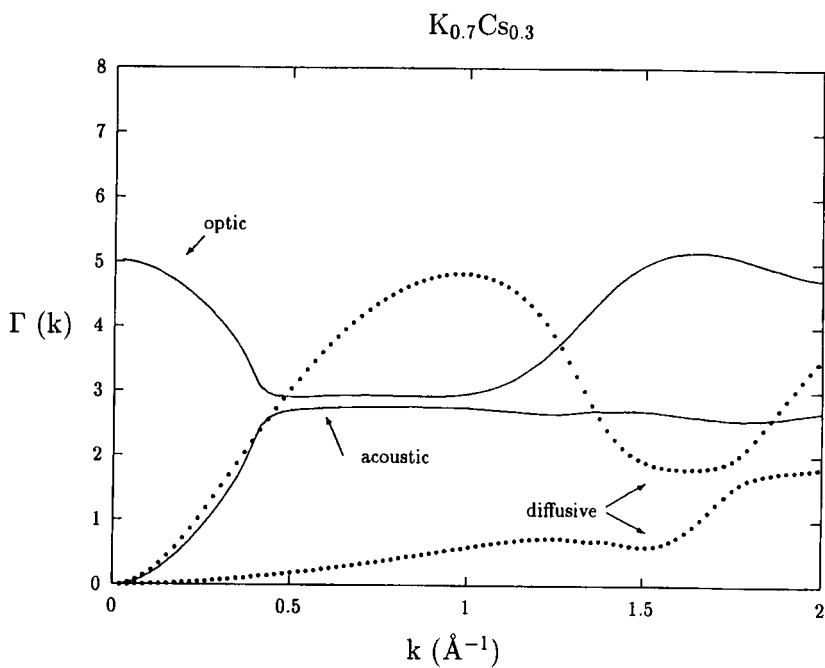


Figure 5 Damping coefficients $\Gamma(k)$ for the $K_{0.7}Cs_{0.3}$ alloy as labeled.

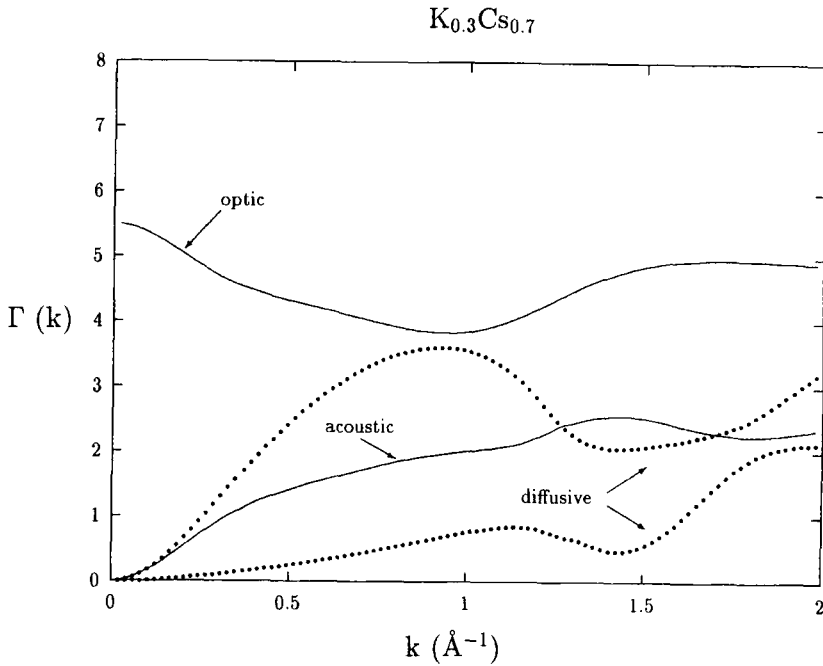


Figure 6 Damping coefficients $\Gamma(k)$ for the $K_{0.3}Cs_{0.7}$ alloy as labeled.

factors for the $K_{0.7}Cs_{0.3}$ alloy at a range of wavevector. The frequencies of the propagating eigenmodes are indicated by an arrow. In the small- k limit, the high-frequency mode is overdamped and makes no visible contribution to the total structure factor. At intermediate wavenumbers ($k \sim 0.3 \text{ \AA}^{-1}$) the eigenfrequencies are very close to each other, and their contributions merge in the single inelastic peak of the total structure factor. Note that $\omega_s^{(1)}(k)$ is associated with a distinct peak in $S_{11}(k, \omega)$ whereas $\omega_s^{(2)}(k)$ causes only a weak shoulder in $S_{22}(k, \omega)$. Both modes are best resolved around $k \sim 1.0 \text{ \AA}^{-1}$ where the contributions from both propagating modes superpose to form a broad plateau at the foot of the quasielastic peak. It is much more difficult to observe the high-frequency mode in the Cs-rich alloy where it manifests itself only in the form of a high-frequency tail of the main inelastic peak (see Fig. 8).

4. DISCUSSION

Although the results presented here indicate some similarities with the fast sound phenomenon, the basic physics are best understood in terms of a simple impurity model. At a majority concentration of the heavier atoms, the starting point is a simple model consisting of a "host" mode following the dispersion relations of the

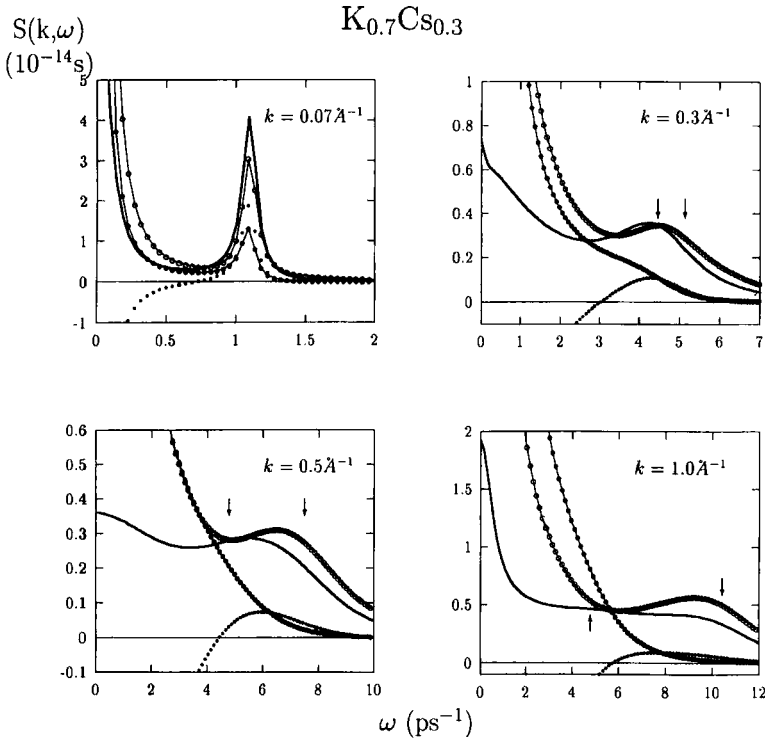


Figure 7 Partial and total (neutron weighted) dynamic structure factors $S(k, \omega)$ and $S_{ij}(k, \omega)$ for $K_{0.7}Cs_{0.3}$ at different wavevectors up to $k = 1.0 \text{ \AA}^{-1}$. Full line – $S(k, \omega)$, \circ – $S_{KK}(k, \omega)$, $-$ $S_{CsCs}(k, \omega)$, $-$ $S_{KCs}(jk, \omega)$. The vertical arrows mark the frequencies of the propagating eigenmodes (cf. text).

pure liquid of the majority species and a dispersion-less high-frequency impurity mode. The slight modulation of the high-frequency impurity mode follows again the dispersion relation of the pure liquid of the lighter atoms. The situation is completely analogous to that found in an analysis of the lattice vibrations of a substitutionally disordered body-centred K_xRb_{1-x} alloy in the range $x = 0.06 - 0.29$, both experimentally by neutron-scattering²⁶ and theoretically via recursion calculations of the phonon-spectrum²⁷. In the limit of an ordered distribution of the impurity atoms, the high-frequency propagating mode becomes the optic mode of the ordered compound. The designation as an optic mode is not entirely inappropriate in the liquid alloy as well, in the sense that mainly the lighter atoms participate in this optic mode. At a majority concentration of the lighter atoms, the impurity mode occurs as a resonance within the frequency-range of the host-vibrations. At the point of intersection between the sound mode of the host-atoms and the stationary impurity mode, the interaction of the two modes lifts the degeneracy, and this immediately leads to the dispersion relations shown in Figure 2. The strong interaction also leads to the strong damping of the high-energy mode in the long-wavelength limit. Again

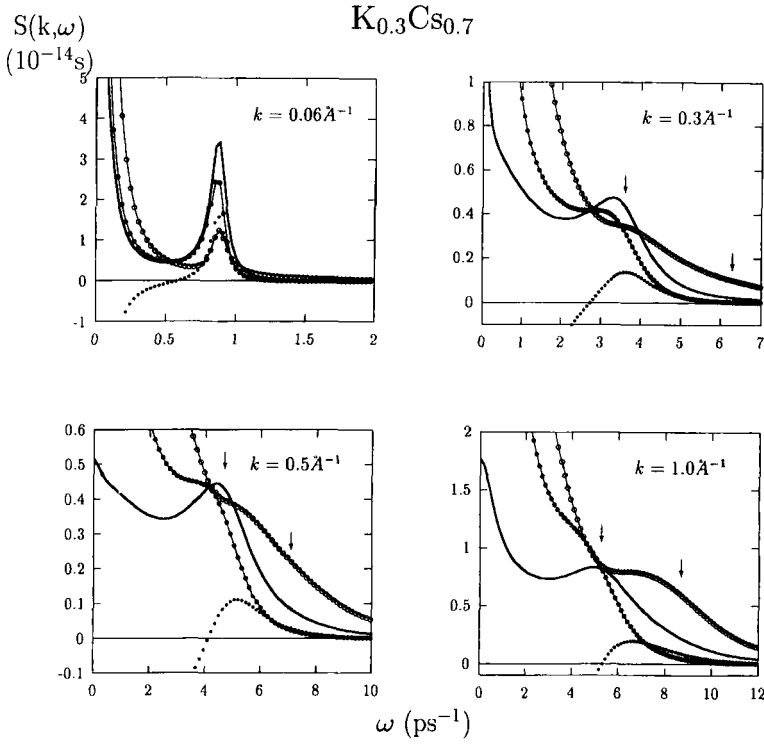


Figure 8 Same as Figure 7, but for $K_{0.3}Cs_{0.7}$.

the situation is completely analogous to that in a substitutional crystalline alloy (see the results on $K_{0.67}Rb_{0.33}$ in Ref.²⁷) and in a glassy $Mg_{0.7}Zn_{0.3}$ alloy²⁸. For the glassy alloy, the theoretical predictions have been verified by inelastic neutron scattering experiments²⁹, although only recently neutron Brillouin-scattering experiments have made it possible to verify the existence of both the high- and low-energy eigenmodes^{30,31}.

The question is now: How does this scenario relate to the fast sound phenomenon? Is there a continuous transition between the long-wavelength behaviour of our optic mode and the fast sound mode, or is fast sound an entirely new phenomenon? Figure 9 shows the dispersion relations for the hypothetical cases where the mass of the heavy atoms has been increased by a factor 3, respectively 10, relative to Cs. We find that—as expected—the frequency of the low-energy mode $\omega_s^{(1)}(k)$ decreases, whereas the high-energy mode $\omega_s^{(2)}(k)$ is nearly unaffected. The damping of the low-energy mode decreases, whereas the damping of the high-energy mode remains as strong as at lower mass-ratios. The dispersion-relations $\omega_i^{ii}(k)$, $i = K$ or Cs and $\omega_i(k)$ derived from the current correlation functions show a curious behaviour: at low k they are determined by the low-energy, at larger k by the high-energy

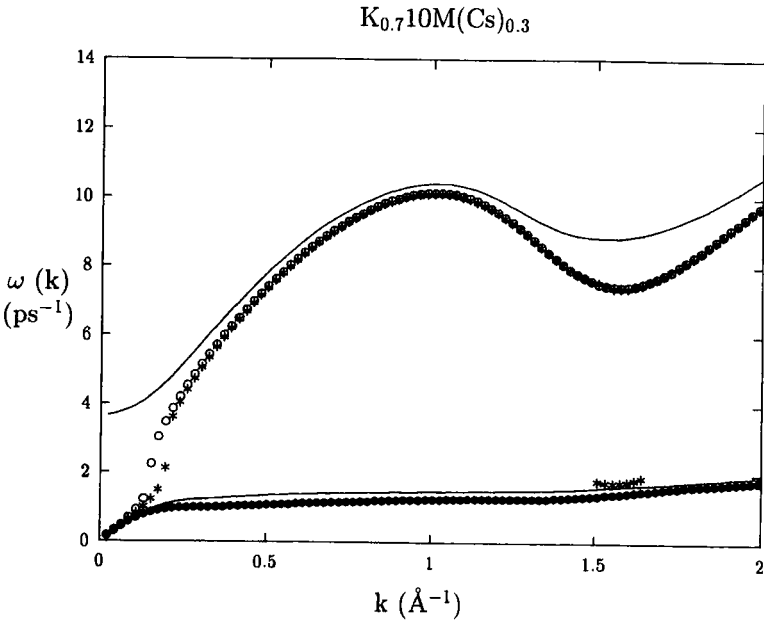
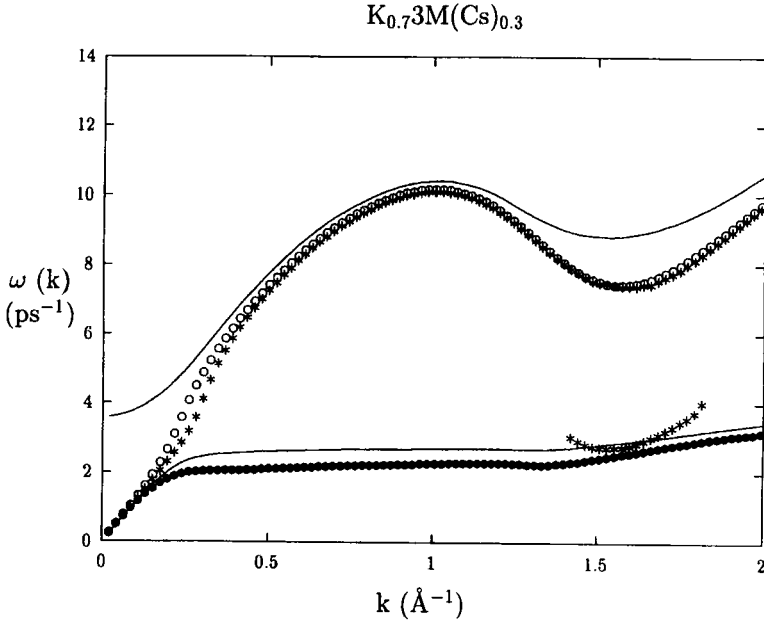


Figure 9 Dispersion relations $\omega_s^{(j)}(k), j = 1, 2$ and $\omega_l^{(i)}(k), i = K, Cs$ for a “ $K_{0.7}Cs_{0.3}$ ” alloy, but with the mass of the “Cs”-particles increased by a factor 3(a), respectively 10(b) (for symbols cf. Fig. 3 and text).

Downloaded At: 08:12 28 January 2011

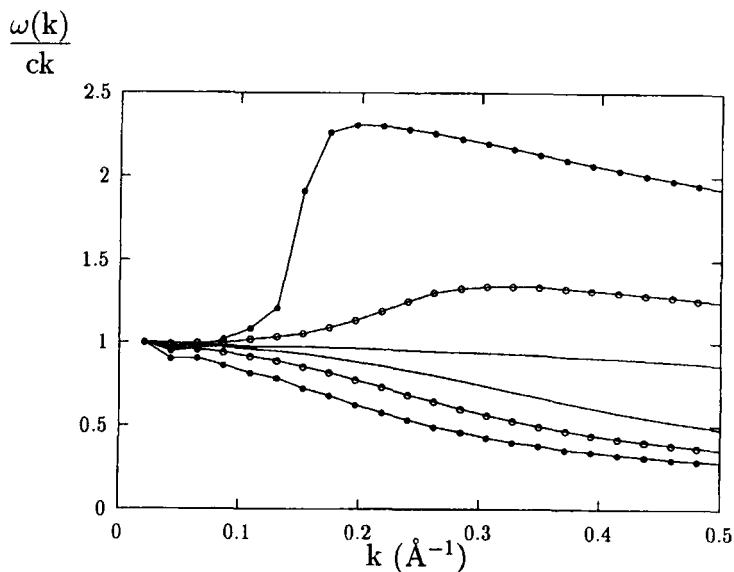


Figure 10 Reduced dispersion relations $\bar{\omega}_l^j(k) = \omega_l^j(k)/ck$, $j = K, Cs$. — mass-ratio = 34, o — mass-ratio = 10.2, full lines — mass-ratio = 3.4; upper curves — K, lower curves — Cs (for values of c cf. text).

mode. In the transition region the Cs-Cs mode shows a negative dispersion. Above the transition region the oscillations of the lighter particles are more or less completely decoupled from the motions of the heavier atoms. If we define reduced dispersion relations $\bar{\omega}_l^i(k) = \omega_l^i(k)/ck$ where c is the hydrodynamic velocity of sound we find that the dispersion relations of the slow and the fast modes merge with the hydrodynamic sound mode in the long-wavelength limit (for the c we find for the $K_{0.7}Cs_{0.3}$ alloys the values 1740 ms^{-1} , 1185 ms^{-1} and 767 ms^{-1} , corresponding to the "normal" Cs mass and to the increased Cs-masses by factors of 3 and 10, respectively). Only at larger wavevectors the two modes separate and slow and fast modes are observed (Fig. 10). We find that the onset of fast sound is shifted to larger k with a decreasing value of the mass-ratio, but there is no change in the essential physics. This result agrees with the light-scattering observations of Wegdam *et al.*³² on H_2/Ar -mixtures at different densities. They showed that fast sound is observed only above a critical wavevector. For smaller k slow and fast sound merge with the hydrodynamic sound mode.

Hence we find, in agreement with experiment, that there is a continuous transition from the conventional description of the dynamical properties of binary mixtures (whether liquid, glassy or crystalline) to the fast sound scenario. This means that the fast sound mode is in reality rather an optic mode where the light particles move out of phase with the heavy atoms (whose motion becomes very slow at large mass ratios), in contrast to the hydrodynamic sound mode where both species move in phase.

Acknowledgements

This work has been supported by the Österreichische Bundesministerium für Wissenschaft und Forschung under Proj. No. GZ 45.385/2-IV/3A/94, by the National Ukrainian Academy of Sciences, and by the Österreichische Forschungsfonds under Proj. Nos. P8912 and P11194.

References

1. U. Balucani and M. Zoppi, *Dynamics of the Liquid State* (Oxford: Clarendon, 1994).
2. G. Jacucci and I. R. McDonald, *J. Phys. F(Met. Phys.)* **10**, L15 (1980).
3. M. Soltwisch, D. Quitmann, H. Ruppertsberg and J.-B. Suck, *Phys. Rev., B*, **28**, 5583 (1983).
4. K. Toukan, H. T. J. Reijers, C.-K. Loong, D. L. Price and M.-L. Saboungi, *Phys. Rev., B*, **41**, 11739 (1990).
5. T. Aihara Jr. and T. Masumoto, *J. Phys. (Cond. Matt.)* **7**, 1525 (1995).
6. J. Bosse, G. Jacucci, M. Ronchetti and W. Schirmacher, *Phys. Rev. Lett.*, **57**, 3277 (1986).
7. U. Balucani, G. Ruocco, A. Torcini and R. Vallauri, *Phys. Rev., E*, **47**, 1677 (1993).
8. P. Westerhuijs, W. Montfrooij, L. A. deGraaf and I. M. deSchepper, *Phys. Rev., A*, **45**, 3749 (1992).
9. P. H. K. deJong, P. Verkerk, C. F. deVroeghe, L. A. deGraaf, W. S. Howells and S. M. Bennington, *J. Phys. (Cond. Matt.)* **6**, L681 (1994).
10. A. Campa and E. G. D. Cohen, *Phys. Rev. Lett.*, **61**, 853 (1988).
11. A. Campa and E. G. D. Cohen, *Phys. Rev., A*, **39**, 4909 (1989).
12. A. Campa and E. G. D. Cohen, *Phys. Rev., A*, **41**, 5451 (1990).
13. W. Montfrooij, P. Westerhuijs and I. M. deSchepper, *Phys. Rev. Lett.*, **61**, 2155 (1988).
14. J.-P. Boon and S. Yip, *Molecular Hydrodynamics* (New York: McGraw-Hill, 1980).
15. Ya. Chushak, J. Hafner and G. Kahl, *Phys. Chem. Liquids*, **29**, 159 (1995).
16. S. W. Lovesey, *J. Phys. C (Solid State Phys.)* **C6**, 1856 (1973).
17. M. A. Ricci, D. Rocca, G. Ruocco and R. Vallauri, *Phys. Rev., A*, **40**, 7226 (1989).
18. D. L. Price and J. R. D. Copley, *Phys. Rev., A*, **11**, 2124 (1975).
19. L. Sjögren and A. Sjölander, *J. Phys. C (Solid State Phys.)* **12**, 4369 (1979); L. Sjögren, *J. Phys. C (Solid State Phys.)* **13**, 705 (1980); L. Sjögren, *Phys. Rev., A*, **22**, 2866 (1980); L. Sjögren, *Phys. Rev., A*, **22**, 2883 (1980).
20. G. E. Bacon, *Acta Crystall. A*, **28**, 357 (1972).
21. N. W. Ashcroft, *Phys. Lett.*, **23**, 48 (1966).
22. S. Ichimaru and K. Utsumi, *Phys. Rev., B*, **24**, 7381 (1981).
23. J. Hafner, *From Hamiltonians to Phase Diagrams* (Berlin: Springer, 1987).
24. Y. Rosenfeld, G. Kahl and B. Bildstein (to be published).
25. Y. Rosenfeld, *Phys. Rev. Lett.*, **63**, 980 (1989); Y. Rosenfeld, *J. Chem. Phys.*, **98**, 8126 (1993); Y. Rosenfeld, *Phys. Rev. Lett.*, **72**, 3831 (1994).
26. W. A. Kamitakahara and J. R. D. Copley, *Phys. Rev., B*, **18**, 3772 (1978).
27. G. Punz and J. Hafner, *Z. Physik, B*, **61**, 231 (1985).
28. J. Hafner, *J. Phys. C (Solid State Phys.)* **16**, 5773 (1983).
29. J. B. Suck, H. Rudin, H. J. Guntherodt and H. Beck, *Phys. Rev. Lett.*, **50**, 49 (1983).
30. J. B. Suck, P. A. Egelstaff, R. A. Robinson, D. S. Sivia and A. D. Taylor, *Europhys. Lett.*, **19**, 207 (1992).
31. C. J. Benmore, B. J. Olivier, J. B. Suck, R. A. Robinson and P. A. Egelstaff, (to be published).
32. G. H. Wegdam, A. Bot, R. P. C. Schram and H. M. Schaink, *Phys. Rev. Lett.*, **63**, 2697 (1989).